Development of Integrated Terahertz Broadband Detectors Utilizing Superconducting Hot-Electron Bolometers

Lei Liu, *Member, IEEE*, Haiyong Xu, *Member, IEEE*, Rebecca R. Percy, *Student Member, IEEE*, Delbert L. Herald, Arthur Weston Lichtenberger, Jeffrey L. Hesler, *Member, IEEE*, and Robert M. Weikle, II, *Senior Member, IEEE*

***Abstract*—We report on the development of terahertz broadband detectors utilizing superconducting hot-electron bolometers and planar sinuous antennas. In this work, sinuous antennas designed to cover the frequency range of 50 GHz to nearly 900 GHz have been fabricated on semi-insulating silicon substrates. To maintain a self-complementary structure, four antenna arms are used, leading to a frequency-independent input impedance of 74 Ω. Two squares of superconducting niobium HEBs are required at the feed point of the antennas as the sheet resistance of a 10 nm thick niobium thin film is 35 Ω/square. Two sizes of HEBs (120 nm × 240 nm, and 2 μm × 4 μm) have been fabricated using e-beam lithography (EBL), and standard photolithography processes, respectively. A quasi-optical mount with high-resistivity silicon lens has been employed for coupling input power to the sinuous antenna. With a close-cycled cryocooler, the detector performance is studied and evaluated. Detector responsivity at 585 GHz has been presented and compared to waveguide Schottky diode detectors. Noise equivalent power (NEP) measurement is discussed and will be soon performed to the detectors developed in this paper.**

***Index Terms*—Detector, hot electron bolometer, sinuous antenna, terahertz.**

I. Introduction

TERAHERTZ (THz) detection technology is becoming more attractive for its applications in astronomy, imaging and bio-sensing [1], [2]. Although waveguide detectors employing Schottky diodes are widely used, they tend to have narrow bandwidths and relatively low sensitivities [3]. Moreover, the impedance mismatch between zero-bias Schottky diodes and waveguide embedding structures are substantial, resulting in a limited power coupling efficiency. Superconducting HEBs have been shown to exhibit higher sensitivity than Schottky diodes at terahertz frequencies [4], [5]. Because HEB devices can be designed to have negligible inductance and capacitance up to THz frequencies, they have the potential for broadband operation when integrated with quasi-optical structures such as self-complementary planar antennas.

In this work, planar sinuous antennas that designed to cover the frequency range of 50 GHz to nearly 900 GHz have been fabricated on semi-insulating silicon substrates. To maintain a self-complementary structure, four antenna arms are used, leading to a frequency-independent input impedance of 74 Ω. Two squares of superconducting niobium HEBs are required at the feed point of the antennas as the sheet resistance of a 10 nm thick niobium thin film is 35 Ω/square. Two sizes of HEBs (120 nm × 240 nm, and 2 μm × 4 μm) have been fabricated using e-beam lithography (EBL), and standard photo-lithography processes, respectively. A quasi-optical mount with high-resistivity silicon lens has been employed for coupling input power to the sinuous antenna. With a close-cycled cryocooler, the detectors performance is studied and evaluated. Detector responsivity at 585 GHz has been presented and compared to waveguide Schottky diode detectors. Noise equivalent power (NEP) measurement is discussed and will be soon performed to the detectors developed in this paper.

II. Detector Design

A. Sinuous Antenna and Quasi-Optical Design

For broadband operation, planar sinuous antenna has been chosen for the detector design [6]. As shown in Fig. 1(a), the four-arm sinuous antenna has a self-complementary log-periodic structure. For each sinuous curve defining the antenna arms, the angular breadth α and offset parameter δ are 45° and 22.5°, respectively. The antenna is fabricated on silicon substrate of 0.5 mm thick and mounted on an extended hemispherical high-resistivity ($\geq$ 1000 Ω · cm) silicon lens ($\varepsilon_{\mathrm{r}} = 11.8$). As shown in Fig. 1(b), the lens radius is 5 mm (chosen to be 10 times of the antenna active radius at 50 GHz) and the total extension length is 1 mm. According to [7], most of the power is radiated into the dielectric side (see Fig. 1(a)). The use of silicon substrate with high dielectric constant enhances the power coupling efficiency for a receiving antenna. In addition, using the same material for both the substrate and lens eliminates the power loss to substrate modes [8].

In this detector design, two of the antenna arms are connected to DC outputs, and the other two arms are suspended to maintain

Manuscript received August 17, 2008. First published ; current version published July 10, 2009. This work was supported by the U.S. Army National Ground Intelligence Center Grant W911W5-06-R-0001.

L. Liu, H. Xu, R. R. Percy, D. L. Herald, A. W. Lichtenberger, and R. M. Weikle, II are with the School of Engineering and Applied Science, University of Virginia, Charlottesville, VA 22904-4743 USA (e-mail: LL8j@virginia.edu; hx4g@virginia.edu; rrp4d@virginia.edu; arthurW@virginia.edu; rmw5w@virginia.edu).

J. L. Hesler is with Virginia Diodes, Inc. (VDI), Charlottesville, VA 22902-6172 USA (e-mail: hesler@vadiodes.com).

Digital Object Identifier 10.1109/TASC.2009.2018268

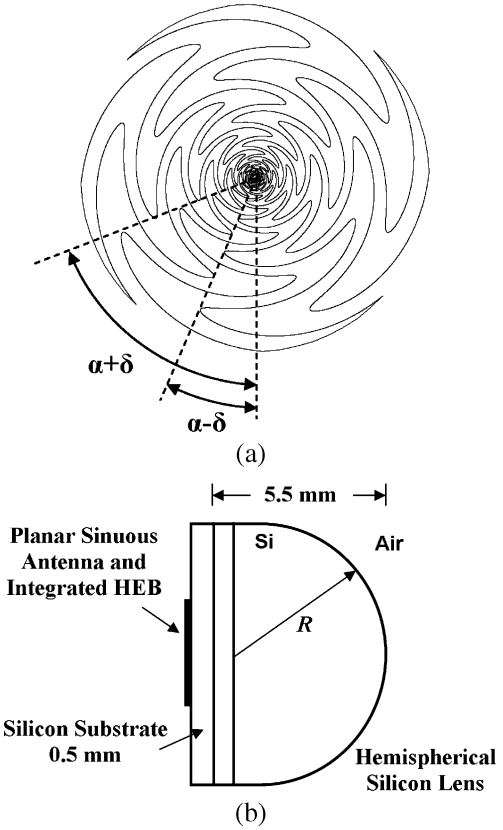

Fig. 1. Broadband THz detector design: (a) the four-arm planar sinuous antenna with self-complementary structure and (b) the planar sinuous antenna mounted on an extended hemispherical silicon substrate lens with radius R, of 5 mm.

a self-complementary structure. The antenna input impedance is then frequency-independent [9], and described by,

$$Z_{ant} = \frac{189\ \Omega}{\sqrt{(\varepsilon_{r\_si}+1)/2}} \tag{1}$$

where 189 Ω is the impedance of any self-complementary structure in free space, and the dielectric constant for silicon is 11.8, resulting in an input impedance of $\sim 74\ \Omega$ for the sinuous antenna shown in Fig. 1(a).

DuHamel has shown that the active region radians for sinuous antennas is given by [6],

$$r \approx \frac{\lambda_e}{4(\alpha+\delta)} \tag{2}$$

where λ_{e} is the effective wavelength and the angles α and δ are in radius. The sinuous antenna designed has the maximum and minimum active radians of 1.5 mm and 30 μm, respectively. It is expected to cover the frequency range of 50 GHz to nearly 900 GHz according to (2). Since HEB devices are in the nano-meter scale, and can be designed to have negligible inductance and capacitance up to several THz, this HEB detector design has the potential to be scaled up to cover much higher frequency range [10].

Compared to other broadband planar antenna designs such as log-periodic antennas and spiral antennas, the polarization of the sinuous antenna is approximately fixed with a wobble of only ±5° [11], which greatly simplifies the detector operation. The dual polarization of this antenna also leads to many other THz applications, for example, frequency multipliers [12].

B. HEB Devices

As discussed in the previous section, the sinuous antenna designed has a frequency-independent input impedance of $\sim 74\ \Omega$. According to [13], the sheet resistance of a 10 nm thick niobium thin film at the normal-state is 35 Ω/square. For optimal power coupling, nearly two squares of superconducting Nb ($\sim$ 70 Ω) are required at the feed point of the sinuous antenna for impedance matching. Similar THz detectors employing zero-bias Schottky diodes have limited power coupling efficiency due to the substantial impedance mismatch between diodes and waveguides/planar antennas, resulting in relatively lower responsivity [3], [14].

Superconducting HEBs have a very sharp dR/dT slope around the critical temperature. The heat capacity of electron subsystem is much smaller than that of the lattice phonons. At low temperature, coupling between the electrons and lattice is relatively weak so that absorbed RF energy initially heats only the electrons. Because coupling to the lattice phonons is weak, the lattice does not contribute much to the overall specific heat of the device, thus allowing faster cooling and broader bandwidth operation. This also results in a higher possible sensitivity. The sensitivity limit of a HEB detector, described by noise-equivalent power level (NEP) due to thermal fluctuation noise is given by [15],

$$NEP = \sqrt{4k_B T^2 G} \tag{3}$$

where $\mathrm{k_B}$ is the Boltzmann constant, T is the electron temperature and G is the thermal conductance between electrons and phonons ($\mathrm{G_{e-ph}}$) for the large devices (2 $\mu\mathrm{m} \times 4\ \mu\mathrm{m}$), or thermal conductance associated with the outdiffusion of hot electrons into the contacts ($\mathrm{G_{e-e}}$) for the nano-scale devices (120 nm × 240 nm). Based on superconducting HEBs, extremely sensitive detectors have been achieved, with the state-of-the-art NEP of $10^{-20}\ \mathrm{W}/\sqrt{\mathrm{Hz}}$ [16]. By integrating nanoscale niobium HEBs (working at ∼4.2 K) with planar sinuous antennas, broadband THz detectors with both high responsivity and low NEP would be expected.

III. Detector Fabrication and Assembling

The detector circuits were fabricated in the Microfabrication Laboratory at the University of Virginia (UVML). For impedance matching, two sizes of HEB devices have been designed and fabricated. The fabrication starts from the sputtering of Nb/Au (10 nm/10 nm) bilayer, followed by definition of the base layer containing sinuous antennas using lift-off process. Larger devices with the dimensions of 2 $\mu\mathrm{m} \times 4\ \mu\mathrm{m}$ have been implemented using standard photolithography process for proof-of-concept design. The larger devices are easier to make and can be used in many applications such as THz spectroscopy and reflectometer although they are expected to have higher NEP. The nano-scale devices with dimension of 100 nm × 200 nm were fabricated with e-beam lithography (EBL) process described in [17]. Typical fabrication results are shown in Fig. 2. The measured device length is 180 nm and the width is

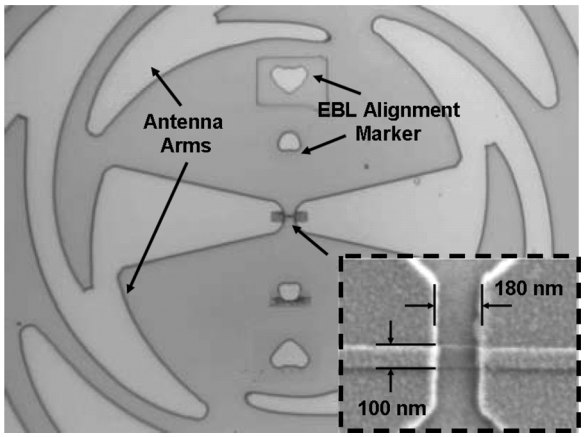

Fig. 2. Fabrication results of the THz broadband detectors utilizing planar sinuous antenna integrated with nano-scale HEB device of 100 nm × 180 nm.

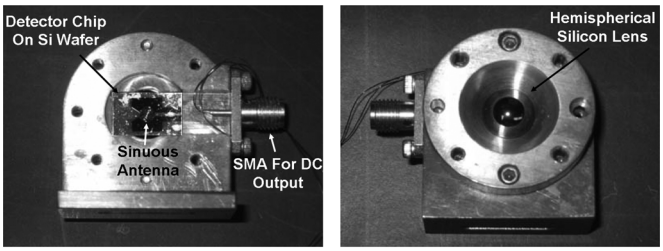

Fig. 3. Broadband HEB THz detector assembling: (a) the backside of the cryogenic mount and (b) the front side showing the hemispherical silicon lens.

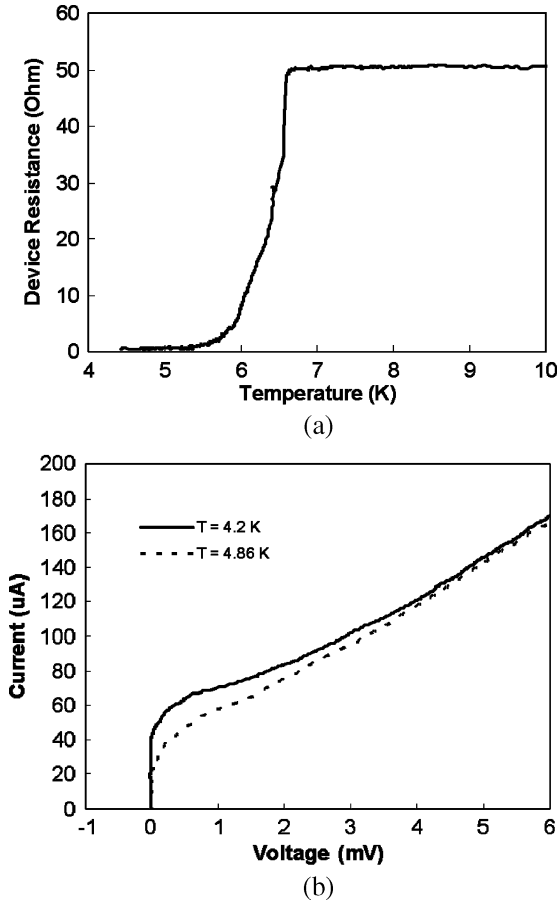

Fig. 4. Typical DC characteristics of the fabricated nano-scale HEB devices: (a) $R-T$ curve shows critical temperature of 5.9 K and transition width of 0.8 K, (b) $I-V$ curves measured at 4.2 K and 4.86 K, respectively.

100 nm, resulting in a HEB resistance of $\sim 64\ \Omega$ at the normal state, which is quite close to the antenna input impedance. The EBL process strongly depends on the operator's skills and quite time-consuming. The "suspended sidewall nano-patterned stencil" (SSNPS or Ti-line) technique has been developed at the University of Virginia [18]. This process does not rely on expensive e-beam or ion-beam facilities, allowing more research organizations to make and test HEB devices. This technique will be used in this research in the future.

A quasi-optical cryogenic mount with high-resistivity silicon lens has been employed for coupling input power to the sinuous antenna. A total extension length of 1.0 mm is chosen for good antenna directivity while maintaining a high Gaussian coupling efficiency [19]. As shown in Fig. 3, the fabricated detector circuit is mounted to the extended hemispherical silicon lens using cryogenic epoxy. The DC signal is output through a standard SMA connector. This quasi-optical mount with detector circuit will be installed into a close-cycled cryocooler (4.0 K) for performance characterization.

IV. Detector Characterization

A. DC Measurement

Prior to RF testing, DC characteristics of the HEB devices have been tested using the dip-stick four-point measurement. Typical results are shown in Fig. 4. The device resistances for this batch are in the range of 50 Ω to 65 Ω, which is slightly less than the 70 Ω designed value. This might be caused by the de-focusing during the EBL process. The $R-T$ curve measured with bias current of 10 μA shows that the superconducting transition occurs at $T_c \sim 5.9$ K with a broad transition width of $\Delta Tc \sim 0.8$ K. The $I-V$ curve measured at a bath temperature of 4.2 K exhibit a critical current of 70 μA. When the bath temperature is increased from 4.2 K to 4.86 K, the critical current decreases from 70 μA to 55 μA as expected.

B. Antenna Characterization

To demonstrate the broadband properties of the designed sinuous antenna, we mounted zero-bias Schottky diode (VDI courtesy) onto the antenna feed point. Although the Schottky diode detector is not optimized, a voltage responsivity of 300–1000 V/W has been measured over the frequency range of 150–440 GHz [14]. The far-field radiation patterns of the sinuous antenna mounted on hemispherical silicon lens have been measured at 196 GHz and 585 GHz. In this measurement, VDI frequency extension modules (FEMs) were utilized for providing the THz radiation. The detector was mounted at a computer-controlled rotation stage and the output DC signal was chopped and detected by a lock-in amplifier. As shown in Fig. 5, the patterns show decent Gaussian-shape main beam with side-lobe level less than −7 dB. The 3-dB beam width at 196 GHz is 10.4°, and decreases to 4.6° at 585 GHz. The sinuous antenna pattern within the dielectric half-space should be frequency—independent. However, the silicon lens utilized acts as an aperture with

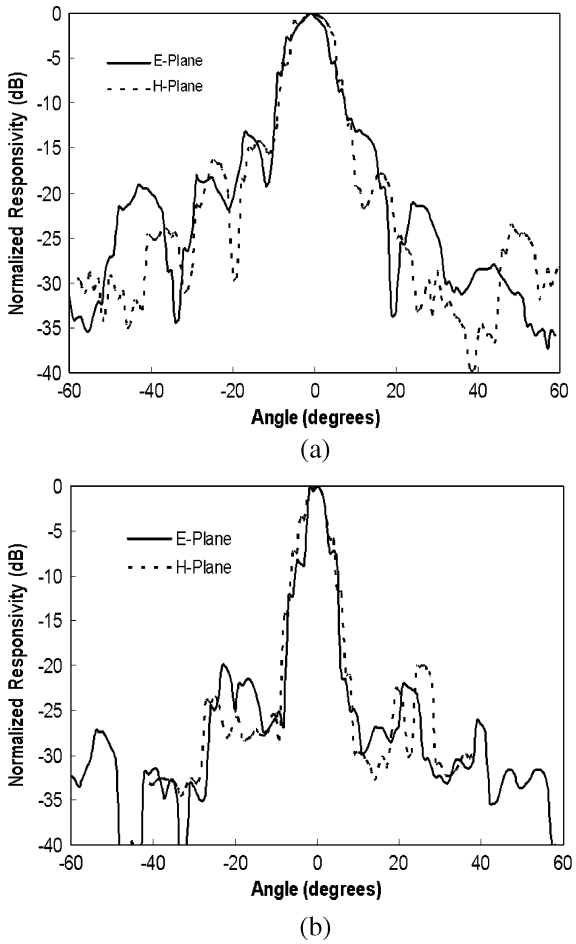

Fig. 5. Measured far-field radiation patterns for the planar sinuous antenna on extended hemispherical silicon lens: (a) antenna patterns measured at 196 GHz and (b) antenna patterns measured at 585 GHz.

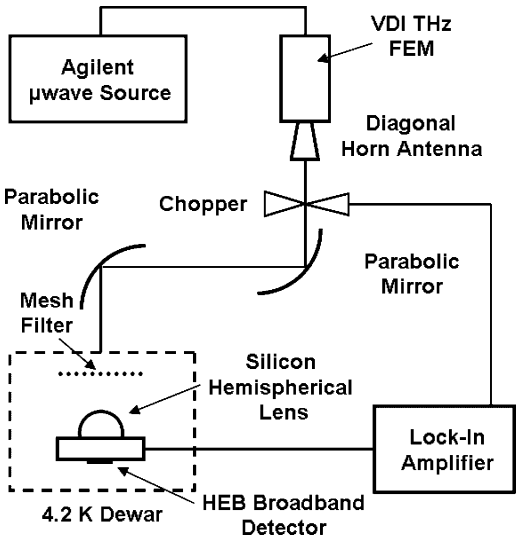

Fig. 6. Diagram of the responsivity measurement setup for the HEB broadband THz detectors.

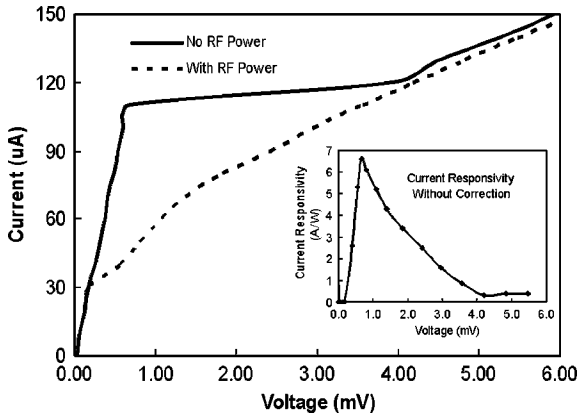

Fig. 7. Responsivity measurement results at 585 GHz for HEB broadband THz detectors. The HEB device (nano-scale) measured has a normal-state resistance of approximately 50 Ω.

fixed dimension, resulting in narrower antenna beam at higher frequencies. The measured H-plane radiation pattern is slightly broader than the pattern in the E-plane, for both 196 GHz and 585 GHz.

C. Detector Responsivity Measurement

The detector responsivity measurement setup for 585 GHz is shown in Fig. 6. An Agilent microwave source together with a VDI 575–635 GHz FEM are employed to provide the THz radiation through a diagonal horn antenna. The HEB THz broadband detector is installed into a close-cycled cryocooler with 3.9 K capability. A VDI 585 GHz mesh filter with 100 GHz bandwidth is placed at the 40 K stage between the Teflon cryocooler window and the detector. Two off-axis parabolic mirrors $(f = 76.4\,\mathrm{mm})$ are utilized to couple the THz radiation onto the HEB detector. The HEB device is biased and the DC signal is output through a bias-T for external processing.

Fig. 7 shows the results for detector responsivity measurement at 585 GHz. The HEB device for this measurement has a normal-state resistance of approximately $50\,\Omega$. The I–V curves with and without THz radiation are measured at a bath temperature of 3.9 K. The current change (ΔI) varies with voltage biasing from zero to 67 μA. The available THz radiation power at the Teflon window is nearly 10 μW. The current responsivity (A/W) is then calculated and plotted in the inset of Fig. 7. A current responsivity of 6.7 A/W (or ∼300 V/W) without correction has been achieved with 0.8 mV biasing. This result is comparable to that for a Schottky-diode based detector reported in the literature [20].

V. Discussion and Conclusion

On the basis of the measured $I - V$ curves in Fig. 7, the RF power coupled onto the HEB device is estimated to be 150 nW. The intrinsic responsivity could be as high as 400 A/W or 2×10^4 V/W, which is similar to the results reported in [21]. Coupling losses are introduced by the Teflon window, mesh filter, silicon lens and substrate. Reflection loss at the air-silicon interface can be reduced by anti-reflection coating, which, however makes the detector narrow bandwidth. Misalignment between the antenna and the silicon lens could introduce as high

as 10-dB loss. This can be improved by employing self-alignment markers (e.g. a circular recess) at the back side of the antenna substrate. The measurement setup shown in Fig. 6 can be optimized to further improve the responsivity measurement.

Another important detector parameter is the NEP which quantifies the noise level generated by the detector itself. NEP also sets a lower limit of the power that can be detected. To estimate the NEP of a detector, tangential signal sensitivity (TSS) measurement is most commonly performed, which sets the input power level to where the noise peaks without RF signal are at the same level as the lowest noise with RF signal. The detector NEP is then related to TSS by, $\mathrm{NEP} = \mathrm{TSS}/(2.8\sqrt{\Delta f})$ [22]. This measurement will soon be performed to the HEB broadband THz detectors developed in this paper.

ACKNOWLEDGMENT

The authors thank all the colleagues from the UVML and the Microwave Lab at the University of Virginia. The authors are also grateful for the assistance and advice of Professors Acar Işın and Bascom S. Deaver, Jr., both with the Department of Physics at the University of Virginia, Charlottesville, VA.

REFERENCES

[1] J. Zmuidzinas and P. L. Richards, "Superconducting detectors and mixers for millimeter and submillimeter astrophysics," *Proceedings of the IEEE*, vol. 92, no. 10, pp. 1597–1616, 2004.

[2] D. Mittleman, M. Gupta, R. Neelamani, R. Baraniuk, J. Rudd, and M. Koch, "Recent advances in terahertz imaging," *Appl. Physics B*, vol. 68, pp. 1085–1094, 1999.

[3] J. L. Hesler and T. W. Crowe, "Responsivity and noise measurements of zero-bias Schottky diode detectors," in *18th Intl. Symp. Space Terahertz Techn.*, Pasadena, March 2007.

[4] D. E. Prober, "Superconducting terahertz mixer using a transition-edge microbolometer," *Appl. Phys. Lett.*, vol. 62, pp. 2119–2121, 1993.

[5] B. S. Karasik, M. C. Gadis, W. R. McGrath, B. Bumble, and H. G. LeDuc, "A low-noise 2.5 THz superconductive Nb hot-electron mixer," *IEEE Trans. Appl. Supercon.*, vol. 7, no. 2, pp. 3580–3583, Jun. 1997.

[6] R. H. DuHamel, "Dual Polarized Sinuous Antennas," European Patent Application 0198575, Feb. 19, 1986, U.S. Patent 702042, Feb. 19, 1985.

[7] D. B. Rutledge, D. P. Neikirk, and D. P. Kasilingham, "Integrated circuit antennas," in *Infrared and Millimeter Waves*, K. J. Button, Ed. New York: Academic Press, 1983, vol. 10, pp. 1–90.

[8] D. B. Rutledge and M. S. Muha, "Imaging antenna arrays," *IEEE Trans. Antennas Propagat.*, vol. AP-30, no. 4, pp. 535–540, July 1982.

[9] Y. Mushiake, "Self-complementary antennas," *IEEE Antennas and Propagation Magazine*, vol. 34, no. 6, pp. 23–29, Dec. 1992.

[10] A. D. Semenov and H. Richter *et al.*, "Terahertz performance of integrated lens antennas with a hot-electron bolometer," *IEEE Trans. Microwave Theory & Tech.*, vol. 55, no. 2, Feb. 2007.

[11] K. M. P. Aghdam, R. Faraji-Dana, and J. Rashed-Mohassel, "The sinuous antenna—A dual polarized feed for reflector-based searching systems," *Int. J. Electron. Commun*, vol. 59, pp. 392–400, 2005.

[12] M. J. DeVincentis, S. Ülker, and R. M. Weikle, II, "A balanced HEMT doubler for quasi-optical applications," *IEEE Microwave and Guided Wave Lett.*, vol. 9, no. 6, Jun. 1999.

[13] R. B. Bass, "Hot-Electron Bolometers on Ultra-Thin Silicon Chips With Beam Leads for a 585 GHz Receiver," Ph.D. dissertation, University of Virginia, , May 2004.

[14] J. L. Hesler, L. Liu, H. Xu, and R. M. Weikle, II, "The development of quasi-optical THz detectors," in *33rd International Conference on Infrared, Millimeter, and Terahertz Waves (IRMMW)*, Pasadena, California, USA, Sep. 2008.

[15] P. L. Richards, "Bolometers for infrared and millimeter waves," *J. Appl. Phys.*, vol. 76, no. 1, July 1994.

[16] J. Wei, D. Olaya, B. S. Karasik, S. V. Pereverzev, A. V. Sergeev, and M. E. Gershenson, "Ultrasensitive hot-electron nanobolometers for terahertz astrophysics," *Nature Nanotech.*, no. 3, pp. 496–500, July 2008.

[17] L. Liu, Q. Xiao, H. Xu, J. C. Schultz, A. W. Lichtenberger, and R. M. Weikle, II, "Design, fabrication and characterization of a submillimeterwave niobium HEB mixer imaging array based on the reverse-microscope concept," *IEEE Trans. Appl. Supercon.*, vol. 17, no. 2, pp. 407–411, Jun. 2007.

[18] J. C. Schultz, J. Z. Zhang, and A. W. Lichtenberger, "Nanoscale superconducting THz hot electron bolometers fabricated with UV lithography on ultra-thin Si beam lead chips," *IEEE Trans. Appl. Supercon.*, vol. 15, no. 2, pp. 480–483, Jun. 2005.

[19] D. F. Filipovic, S. S. Gearhart, and G. M. Rebeiz, "Double slot antennas on extended hemispherical and elliptical silicon dielectric lenses," *IEEE Trans. Microwave Theory & Tech.*, vol. 41, pp. 1738–1749, Oct. 1991.

[20] C. Sydlo, O. Cojocari, D. Schönherr, T. Göbel, S. Jatta, H. L. Hartnagel, and P. Meissner, "Ultrawideband THz detector based on a zero bias Schottky diode," in *19th Intl. Symp. Space Terahertz Techn.*, Groningen, April 2008.

[21] D. F. Santavicca, M. O. Reese, A. B. True, C. A. Schmuttenmaer, and D. E. Prober, "Antenna-coupled niobium bolometers for terahertz spectroscopy," *IEEE Trans. Appl. Supercon.*, vol. 17, no. 2, pp. 412–415, July 2007.

[22] A. M. Cowley and H. O. Sorensen, "Quantitative comparison of solid-state microwave detectors," *IEEE Trans. Microwave Theory & Tech.*, vol. MTT-14, pp. 588–602, Dec. 1966.